arXiv:1109.2470v1 [quant-ph] 12 Sep 2011

Inherent Mach-Zehnder interference with "which-way" detection for single particle scattering in one dimension

Lan Zhou,[1] Yue Chang,[2] H. Dong,[2] Le-Man Kuang,[1] and C. P. Sun[2,*]

[1] *Key Laboratory of Low-Dimensional Quantum Structures and Quantum Control of Ministry of Education, and Department of Physics, Hunan Normal University, Changsha 410081, China*

[2] *Institute of Theoretical Physics, Chinese Academy of Sciences, Beijing, 100190, China*

We study the coherent transport of single photon in a one-dimensional coupled-resonator-array, "non-locally" coupled to a two-level system. Since its inherent structure is a Mach-Zehnder interferometer, we explain the destructive interference phenomenon of the transmission spectrums according to the effect of which-way detection. The quantum realization of the present model is a nano-electromechanical resonator arrays with two nearest resonators coupled to a single spin via their attached magnetic tips. Its classical simulation is a waveguide of coupled defected cavity array with double couplings to a side defected cavity.

PACS numbers: 03.65.Xp, 03.65.Yz, 42.50.Ct

I. INTRODUCTION

In quantum mechanics, the Bohr's complementarity principle for wave-particle duality could be displayed in various double-slit experiments (DSE)[1]. It manifests that a detection about which way a particle takes in DSE will inevitably destroy quantum interferences, thus the particle behavior(spatially localized) emerges while wave-like behavior (interference) disappears. Otherwise, if the detectors (apparatuses or environments) can not well distinguish the different possible paths, the interference recovers[2–4]. Lots of experiments have tested this duality properties through the which-way detection[5–8]. In this paper, we show the effect of which-way detection in a class of experimentally accessible systems with an inherent structure of the Mach-Zehnder interferometer where two virtual paths intrinsically are embedded.

We illustrate this observation with the single particle (photon or phonon) propagating in a one-dimensional coupled-resonator-array (CRA) where a localized two-level system (TLS) simultaneously interacts with the confined EM field modes in two nearest resonators (illustrated in Fig. 1(a)). The transported boson is scattered by the TLS when it enters one of these two nearest resonators, and then the transmission/reflection spectrum will exhibit the interference pattern of the twice scatterings. One may superpose these two local EM modes according to their couplings to the TLS (as illustrated in Fig. 1(b)). Their anti-bonding superposition is decoupled with the TLS, while the only interaction between the bonding superposition and TLS makes a which-way detection for the two virtual paths corresponding to the bonding and anti-bonding modes. In this inherent Mach-Zehnder interferometer with which-way detector by the TLS, as the coupling strength increases gradually, the intrinsic interference in the scattering spectrum (the reflection and transmission spectra) will disappear progressively. The reason is that the which-way detection only observes the particle motion in the anti-bonding branch. Therefore the de-interference phenomenon for a single particle scattering is understood in terms of the inherent Mach-Zehnder interferometer under the intrinsic "which-way" detection, which seems absent in the real configuration.

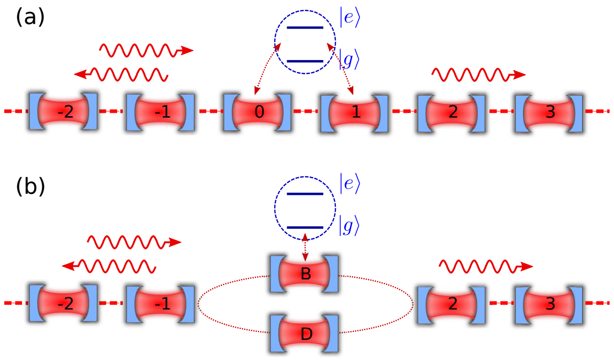

FIG. 1. (Color online) Schematic of the studied system and the physical mechanism. (a) The single boson (photon or phonon) scattered by a nonlocal two-level system simultaneously coupled to two nearest resonators in a one-dimensional coupled-resonator-array (CRA);(b) the equivalent Mach-Zehnder interferometer with which-way measurement where the bonding and anti-bonding superposition of the two local cavity modes form two pathes for interference, one of which is probed by the TLS while another is decoupled with it.

The paper is arranged as follows: In Sec. II, we introduce the model for demonstrating the Mach-Zehnder interference. In Sec. III, we study the single photon propagation properties on this structure. The physical mechanism of the observed phenomena is explored in Sec. IV by taking advantage of the Mach-Zehnder interference. The possible physical realizations the system are discussed in Sec. V. We conclude the paper in Sec. VI.

---

[*] http://power.itp.ac.cn/~suncp; suncp@itp.ac.cn

II. MODEL SETUP

The present system consists of CRA and a side-coupled TLS. In contrast to the previous model[10], the TLS is coupled to two modes supported by two nearest resonators, as illustrated in Fig. 1(a). The CRA is described by the model Hamiltonian under the nearest-neighbor approximation

$$H_C = \sum_j \omega_c a_j^\dagger a_j - \sum_j \xi \left(a_{j+1}^\dagger a_j + \text{H.c.} \right), \tag{1}$$

with the annihilation/creation operator $a_j/a_j^\dagger$ of a confined boson (photon in a single mode cavity or cooled phonon in a nano-mechanical resonator) in the jth resonant cavity mode. This is a typical tight-binding boson model. For simplicity, we assume that all cavities have the same eigenfrequency ω_c and the intercavity coupling has the same strength ξ. In this array, waves propagate freely and are characterized by the dispersion relation

$$\omega_k = \omega_c - 2\xi \cos k, \tag{2}$$

which forms a frequency band in a continuum spectrum.

The TLS with the ground state $|g\rangle$, excited state $|e\rangle$ and energy level-spacing Ω, is coupled to two nearest cavities of the 1D CRA with corresponding strengths g_0 and g_1. Under the rotating-wave approximation, the dynamics of the TLS interacting with the electromagnetic field is described by the Jaynes-Cummings (JC) Hamiltonian

$$H_I = \Omega \sigma_{ee} + \sigma_- \left(g_0 a_0^\dagger + g_1 a_1^\dagger \right) + \text{H.c.}, \tag{3}$$

where the first term describes the free energy of the TLS with $\sigma_{ee} = |e\rangle \langle e|$, and $\sigma_- = |g\rangle \langle e|$ and its adjoint σ_+ are the corresponding lowing and rising operator. We remark that the present model can be physically implemented with nano-electrimechanical resonator array or defect resonator array on photonic crystal. The detailed discription will be presented in Sec. V.

III. SINGLE-PHOTON SCATTERING

It is clear that the number of excitations is conserved in this hybrid system. In the one-excitation subspace, two mutually exclusive possibilities are considered: the particle is either propagating inside the cavity, or absorbed by the TLS. It indicates that the eigenstate has the form

$$|E_k\rangle = \sum_j [u_{kj} a_j^\dagger |0g\rangle + u_{ke} |0e\rangle]. \tag{4}$$

From the Schrödinger equation $(H_C + H_I) |E_k\rangle = E_k |E_k\rangle$, we derive a series of coupled stationary equations for the excited-state amplitude u_{ke} and the amplitudes u_{kj} of single-photon states[10] in the $j - th$ cavity. Here, the part concerning excited-state

$$(E_k - \Omega) u_{ke} = (g_0 u_{k0} + g_1 u_{k1})$$

leads to dispersive coupling strength between the 0th and 1st resonators, and a non-local effective potential

$$V(j) = G(E_k) \left(|g_0|^2 \delta_{j0} + |g_1|^2 \delta_{j1} \right), \tag{5}$$

which is proportional to the Green function $G(E_k) = (E_k - \Omega)^{-1}$. The single excitation transport is described by the discrete scattering equation

$$\begin{aligned} (\omega_c - E_k) u_{kj} =& \xi \left(u_{kj-1} + u_{kj+1} \right) \\ &+ G(E_k) \left(g_j \delta_{j0} + g_j \delta_{j1} \right) \left(g_0 u_{k0} + g_1 u_{k1} \right). \end{aligned} \tag{6}$$

The first term on the right of Eq. (6) charactrizes the hopping between different sites as the kinetic term. And the double delta potentials in the send term are induced from the couplings between the TLS and the CRA. However, such delta potentials are nonlocal comparing with the one-site coupling in Ref. [10]. Therefore, the coherent scattering by the two sites will bring different physical effect.

The process that an incident wave impinges upon the structure, where transmitted and reflected wave emerge, is formulated by assuming

$$u_k(j) = \exp(ikj) + r_k \exp(ikj) \tag{7}$$

for $j \leq -1$ and

$$u_k(j) = t_k \exp(ikj) \tag{8}$$

for $j \geq 2$ with reflection and transmission amplitudes, r_k and t_k. Concerning Eq. (6) to the 0th and 1st resonators with the above assumptions, we immediately obtain the transmission

$$t_k = \frac{2i \sin k \left[(E_k - \Omega) \xi - g_0 g_1 \right]}{2i \sin k \left(E_k - \Omega \right) \xi - 2 g_0 g_1 e^{ik} - (g_1^2 + g_0^2)}, \tag{9}$$

and reflection amplitudes

$$r_k = \frac{2i \sin k g_1^2 e^{ik} + 2 g_0 g_1 e^{ik} + \left(g_1^2 + g_0^2 \right)}{2i \sin k \left(E_k - \Omega \right) \xi - 2 g_0 g_1 e^{ik} - (g_1^2 + g_0^2)}. \tag{10}$$

The eigen-energy $E_k = \omega_k$ is obtained by applying Eq. (6) to the resonators far away from the resonators at $j = -1$ to 2. It is checked that the reflection coefficient $R = |r_k|^2$ and transmission coefficient $T = |t_k|^2$ satisfy the identity $|r_k|^2 + |t_k|^2 = 1$.

It is clear that, in Eq. (9) and (10), the transmission generally vanishes at the band edges with $k = 0, \pi$. However, constructive interference is found at $k = \pi$ when $g_0 = g_1 = g$ (red solid line in Fig. 2). Compared with the case of one-site coupling (solid dotted line in Fig. 2), the transmission does not vanishes at $E_k = \Omega$ with a nonvanishing amplitude

$$t_k = \frac{2i g_0 g_1 \sin k}{2 g_0 g_1 \exp(ik) + (g_1^2 + g_0^2)}, \tag{11}$$

due to the "non-local" coupling between the TLS and CRA. Obviously, the position of transmission zero is shifted to $\Omega + g_0 g_1/\xi$. When the coupling gets stronger, the transmission dip gradually moves outside the spectrum band, thus no transmission zero appears, as shown in Fig. 2. The coupling between the TLS and CRA induces the effective double delta potentials in the way of photon propagation. The strength tends to infinite potentials at $E_k = \Omega$, which indicates the total reflection. However, the straightforward physics picture fails to explain the nonvanishing transmission at $E_k = \Omega$ in the case of nonlocal coupling.

IV. DE-INTERFERENCE AND WHICH-WAY EXPLANATION

To give an intuitionistic explanation about the nonvanishing point of transmission, we now introduce the bonding and anti-bonding modes

$$B = a_0 \cos\theta + a_1 \sin\theta,$$
$$D = -a_0 \sin\theta + a_1 \cos\theta,$$

where $\tan\theta = g_1/g_0$. When $g_0 = g_1 = g$, the modes B and D presents two virtual paths without direct coupling between each other, then the CRA virtually becomes an equivalent Mach-Zehnder interferometer (see the Fig. 1(b)) where the arm B is experienced a which-way measurement by the TLS. Those cavities on the left of the cavity at $j = -1$ or the right of the cavity at $j = 2$ are regarded as the left and right leads, which are connected to each other via two arms. The lower arm corresponds to the anti-bonding model D of eigenfrequency $\omega_D = \omega_c + \xi \sin 2\theta$, while the upper arm to the bonding mode B of eigenfrequency $\omega_B = \omega_c - \xi \sin 2\theta$ coupling to the TLS with coupling strength $\sqrt{2}g$. The effective hopping strengthes between the bonding mode B and nearby cavities are $\xi \cos\theta$ and $\xi \sin\theta$, as shown in Fig. 1(b). It is emphasized that anti-bonding mode D is indeed decoupled with the TLS.

In the above equivalent configuration, the propagating state is a superposition of four mutually exclusive possibilities: i) the particle propagating inside left and right leads, represent by the state $a_j^\dagger |0g\rangle$ with possibility amplitude u_{kj}; ii) absorbed by the TLS, by $u_{ke}|0e\rangle$; iii) propagating from the left to right lead via the upper arm, by $B^\dagger |0g\rangle$ with amplitude u_{kB}, or iv) via the lower am, by $D^\dagger |0g\rangle$ with amplitude u_{kD}. The superposition of these four possibilities forms a stationary state $|E_k\rangle$ with the band energy E_k. Here, three scattering channels are implied, i.e., single particle travels through the excited TLS or via the bonding and anti-bonding branches respectively with the TLS unexcited. In the reduced dimensionality, particles follow two different paths defined by two virtual modes. We refer to these two paths as path B and D corresponding to the B-slit and D-slit. A dispersion delta potential is localized in path B since particle passing the B-slit will interact with the TLS. The total transmission amplitude is the sum of the amplitudes in the two branches, and the interference pattern is determined by the phase difference between the two paths. Therefore, the suppression of quantum interference depends on the dwell time of the single particle absorbed by the TLS.

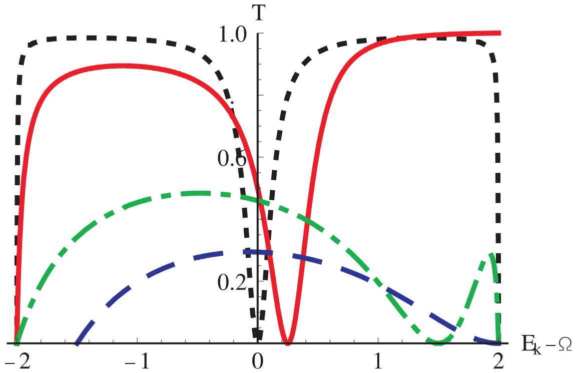

FIG. 2. (Color online) Transmission coefficient T with transition energy $\Omega = \omega_c = 2$ as a function of the photon incident energy E_k . The coupling strengths $g_0 = 0.5, g_1 = 0$ for black dotted line, $g_0 = g_1 = 0.5$ for red solid line, $g_0 = 1, g_1 = 1.5$ for green dot-dashed line, and $g_0 = 1, g_1 = 2.5$ for blue dashed line.

An incoming wave with energy E_k, incident from the left lead, is split into two branches at the first junction and joins again into the outgoing wave at the second junction. The single particle propagating around the ring (consists of sites $-1, D, B, 2$ shown in Fig. 1(b)) is described as follows: the discrete scattering equation in the path B

$$(E_k - \omega_B)\, u_{kB} = \sqrt{2} g u_{ke} - \frac{\xi}{\sqrt{2}} \left(u_{k2} + u_{k-1}\right), \tag{12}$$

which is coupled with the local atomic excitation characterized by

$$(E_k - \Omega)\, u_{ke} = \sqrt{2} g u_{kB};$$

In the path D, the particle propagates freely with motion equation $(E_k - \omega_D)\, u_{kD} = \xi \left(u_{k2} - u_{k-1}\right)/\sqrt{2}$. However, on the nodes with $j = -1, 2$, the amplitudes for the single particle is coupled to those two splitting nodes B and D with the following forms respectively

$$(E_k - \omega_c)\, u_{k-1} = -\xi u_{k-2} - \frac{\xi}{\sqrt{2}} \left(u_{kB} + u_{kD}\right), \tag{13}$$

$$(E_k - \omega_c)\, u_{k2} = \frac{\xi}{\sqrt{2}} \left(u_{kD} - u_{kB}\right) - \xi u_{k3}. \tag{14}$$

Then, it follows from the above discrete scattering equation that the transmission amplitude $t_k = t_k^D + t_k^B$ is given by the partial wave transmission amplitude $t_k^D = i \sin(k/2) \exp(-ik/2)$ and

$$t_k^B = \frac{e^{-ik/2} \xi \left(E_k - \Omega\right) \cos(k/2)}{\xi \left(E_k - \Omega\right) - g^2 + i g^2 \tan^{-1}(k/2)}. \tag{15}$$

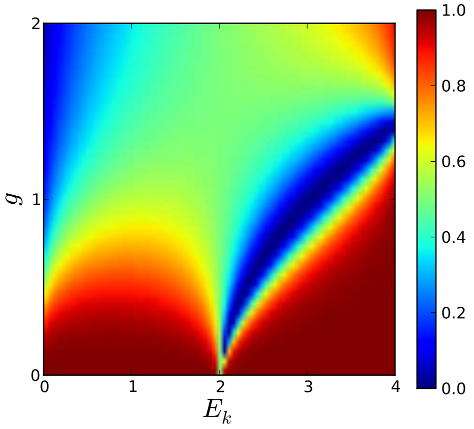

FIG. 3. (Color online) Transmission coefficient $|t_k|^2$. Its contour plot with respect to E_k and coupling strength g. All parameters are in units of ξ.

respectively in path D (B) in the absence of path B (D).

When the incident single particle is resonant to the TLS, the spontaneous emission from the TLS and the propagating modes in the 1D continuum lead to the complete suppression of the wave transmission in path B, then photons take path D. Therefore, the TLS prevents single-particle interference of paths B and D. In this sense, the TLS serves as a which-path detector. It is the potential exerted by the TLS that makes waves accumulate a phase on path B, then the wave interference of paths B and D displays a transmission zero in t_k. However, the coupling strength characterizes the time that the single quantum dwells in the TLS. Consequently, the interference pattern is expected to diminish as the coupling strength increases. Figure 3 shows the contour plots of transmission coefficient $|t_k|^2$ as a function of the incident energy E_k and coupling strength g. Here, we can see that as the coupling strength g increases the complete suppression of the wave transmission begins at $E_k = \Omega$, gradually shifts to the band edge, and then disappears. One may also find that the perfect transmission at $k = \pi$ is independent of the potential exerted by the TLS. When $k = \pi$, the probability amplitudes $u_{kj} = (-1)^j$ for $j \neq 0$, 1, lead to destructive interference at B-slit since $u_{kB} = 0$, and constructive interference at D-slit. In this case, the TLS is effectively decoupled from the CRA.

V. PHYSICAL IMPLEMENTATIONS

The above "non-local" coupling obviously distinguishes the present investigation from previous extensive ones [9–12] where the TLS only couples with the EM field in a single cavity. Experimentally, the previous setups are feasible implemented with the confined photon or the single mode phonon in some confined nanostructures [13], e.g., the circuit QED system, a semiconductor quantum dot coupling with nanoscale surface plasmons or the defect cavities of photonic crystal, and the nano-electromechanical resonator arrays where every resonator is coupled to a localized spin [14]. To implement the present "non-local" coupling seems difficult in the photonic CRA, but it could be feasible for the nano-electromechanical resonator array coupled to a local spin, where two of the resonators are attached by magnetic tips producing magnetic fields in the x-direction (see the Fig. 4). With the charged resonators oscillating in the z-direction, and under the rotating-wave approximation, the inter-resonator coupling is realized via Coulomb forces [14], while two of them simultaneously interacts with a single spin through the magnetic-field gradients [15]. In nano-electromechanical resonator experiments, the parameters ω_c, ξ and Ω can easily reach a million Hertz frequency scale, and the cavity-TLS coupling strength is in the order of 100kHz. The second implementation of the "non-local coupling" could be in a 2D photonic crystal [16], which is made up of a square lattice of high-index dielectric rods, as illustrated in Fig. 4. Here, two nearest cavities in a waveguide of coupled defected cavity arrays is coupled to a side defected cavity. In the single excitation subspace, the side cavity with two states (vacuum and single photon) simulates the TLS in our general setup.

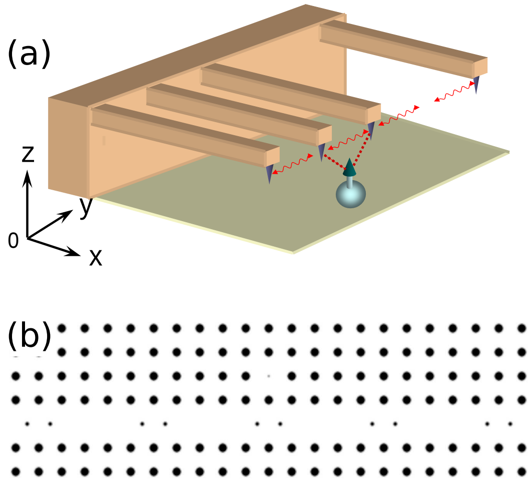

FIG. 4. (Color online)Two physical implementations: (a). Nano-electromechanical resonator arrays where two nearest resonators with ferro-magnetic particles in the tips are coupled to a localized spin. The origin of the coordinate frame is at the spin. Here, all the resonators are charged so that they interact with neighbor ones via Coulomb forces; (b). In the 2D photonic crystal, a side-defected cavity with double couplings to a waveguide of coupled defected cavity arrays. In the single excitation subspace, the side cavity with two states behaves as a TLS.

VI. CONCLUSION

In conclusion, we have studied the effect of which-way detection inherent to a class of experimentally accessible systems with some intrinsic Mach-Zehnder interferometer configuration to enjoy the quantum/classical interference of two virtual paths. This observation is used to explain the discovered progressive de-interference in the transmission spectrum of single photons propagating in 1D CRA, as the non-local couplings of a TLS to two nearest resonators increases its strength gradually. Besides the quantum realizations with the nanoelectromechanical resonator arrays where two nearest resonators with magnetic tips simultaneously interact with a single spin, the classical analogue is proposed based on a waveguide of coupled defected cavity array with double couplings to a side defected cavity.

This work was supported by NSFC through grants 10974209, 10935010, 11074071, and 10775048, the National 973 program (Grant No. 2012CB922103). NCET-08-0682, PCSIRT No. IRT0964, the Project-sponsored by SRF for ROCS, SEM [2010]609-5, and the Key Project of Chinese Ministry of Education (No. 210150).

[1] N. Bohr, in Albert Einstein: Philosopher Scientist (ed. Schilpp, P. A.) 200 (Library of Living Philosophers, Evanston,1949).
[2] W.H. Zurekk, Rev. Mod. Phys. **75**, 715 (2003).
[3] A. Stern, Y. Aharonov, and Y. Imry, Phys. Rev. A **41**, 3436 (1990).
[4] Y. Aharonov, D.Z. Albert, and L. Vaidman, Phys. Rev. Lett. **60**, 1351 (1988).
[5] E. Buks *et al.*, Nature **391**, 871 (1998)
[6] S. Durt, T. Nonn, and G.Rampe, Nature **395**, 33 (1998).
[7] R. Schuster *et al.*, Nature **385**, 417 (1997) .
[8] X.Y. Zou, L. J.Wang, and L. Mandel, Phys. Rev. Lett. **67**, 318(1991).
[9] J.T. Shen and S. Fan, Phys. Rev. Lett. **95**, 213001 (2005).
[10] L. Zhou *et al.*, Phys. Rev. Lett. **101**, 100501 (2008).
[11] L. Zhou,F.M. Hu, J. Lu, and C.P. Sun, Phys. Rev. A **74**, 032102 (2006); L. Zhou, Y.B. Gao, Z. Song, and C.P. Sun, Phys. Rev. A **77**, 013831 (2008). L. Zhou, H. Dong, Y.X. Liu, C.P. Sun, and F. Nori, Phys. Rev. A **78**, 063827 (2008). L. Zhou, S. Yang, Y.X. Liu, C.P. Sun, and F. Nori, Phys. Rev. A **80**, 062109 (2009); J.Q. Liao et al, Phys. Rev. A **81**, 042304 (2010).
[12] O. Astafiev *et al.*, Science **327** , 840 (2010).
[13] J.D. Joannopoulos *et al.*, *Photonic crystals molding the flow of light*, Princeton university press (2008).
[14] P. Rabl *et al.*, Nature Phys. **6**, 602 (2010).
[15] Y. Chang, C.P. Sun, e-print arXiv:1101.2115.
[16] D.Z. Xu, H. Ian, T. Shi, H. Dong and C.P. Sun, Sci. China Phys. Mechanics and Astronomy **53**, 1234 (2010)